Local Order in Aqueous NaCl Solutions and Pure Water: X-ray Scattering and Molecular Dynamics Simulations Study

Salah Bouazizi,[†] Salah Nasr,*[,†] Nejmeddine Jaîdane,[‡] and Marie-Claire Bellissent-Funel[§]

Laboratoire Physico-Chimie des Matériaux, Département de Physique, Faculté des Sciences de Monastir, 5019 Monastir, Tunisia, Laboratoire de Spectroscopie Atomique, Moléculaire et Applications, Département de Physique, Faculté des Sciences, Université Tunis- El Manar, 1060 Tunis, Tunisia, and Laboratoire Léon-Brillouin (CEA-CNRS), CEA Saclay, 91191 Gif-sur-Yvette Cedex, France

Received: July 3, 2006; In Final Form: September 12, 2006

The microstructures of pure water and aqueous NaCl solutions over a wide range of salt concentrations (0−4 m) under ambient conditions are characterized by X-ray scattering and molecular dynamics (MD) simulations. MD simulations are performed with the rigid SPC water model as a solvent, while the ions are treated as charged Lennard-Jones particles. Simulated data show that the first peaks in the O···O and O···H pair correlation functions clearly decrease in height with increasing salt concentration. Simultaneously, the location of the second O···O peak, the signature of the so-called tetrahedral structure of water, gradually disappears. Consequently, the degree of hydrogen bonding in liquid water decreases when compared to pure fluid. MD results also show that the hydration number around the cation decreases as the salt concentration increases, which is most likely because some water molecules in the first hydration shell are occasionally substituted by chlorine. In addition, the fraction of contact ion pairs increases and that of solvent-separated ion pairs decreases. Experimental data are analyzed to deduce the structure factors and the pair correlation functions of each system. X-ray results clearly show a perturbation of the association structure of the solvent and highlight the appearance of new interactions between ions and water. A model of intermolecular arrangement via MD results is then proposed to describe the local order in each system, as deduced from X-ray scattering data.

I. Introduction

Liquid water is certainly the most abundant biological fluid on earth. Despite its simplicity, it presents a large number of specific properties, a good part of which comes from intermolecular hydrogen bonding. It is also well-known that many anomalous properties of water are the consequence of specific H-bond interactions between molecules.[1] Moreover, biological macromolecules such as proteins and nucleic acids adopt their structure and carry out their catalytic roles while interacting with thousands of surrounding water molecules.[2]

In its most common natural shapes, water contains a large variety of dissolved bodies. Then, the investigation of the interactions between water and the solutes on one hand and the interactions between the different molecules or atoms of solutions on the other hand helps in understanding some essential biological mechanisms such as the functional withdrawal of proteins, their identification, and their association in typical fixation processes as ligand−receptor, enzyme−substrate, or antigen−antibody.[3]

Due to their importance in many areas of physical chemistry and molecular physics, several attempts have been made to study aqueous ionic solutions using computer simulations with various water models[4−8] and experimental techniques.[9−12] In particular, Na^+ and Cl^- which are essential for biophysical systems have attracted particular attention. A simple example is the physiological liquid in the human body, containing about 0.8 mol of NaCl, that is, one sodium ion and one chloride ion per 100 water molecules.

Some computational studies about the structural and dynamic aspects of aqueous NaCl solutions were already done.[13,14] Belch et al.[15] have been concentrating their effort on the role played by water in the presence of Na^+, Cl^- ion pair interconversion from solvent-separated into close contact configuration. Degrève et al.[16,17] have analyzed by molecular dynamics (MD) and Monte Carlo (MC) simulations a microscopic study of 1 M aqueous NaCl solution. On one hand, the authors show that the structure of the solution is governed by the properties of the solvent and the features of the ion pairs obey the electrostatic attraction or repulsion and the hydration effects. On the other hand, the stability of the local structures formed by ions was determined by their lifetimes which are estimated for neutral, negatively charged, and positively charged ion pairs. Much less experimental investigations on aqueous NaCl solutions can be found in the literature. Particularly, the characterization of the local order in such solutions, in terms of pair correlation functions or structure factors, is often neglected.

In the present paper and in the course of our systematic study of hydrogen-bonded liquids, we present X-ray scattering data on pure water and aqueous NaCl solutions at various salt concentrations. X-ray diffraction is well adapted to the study of hydration phenomena, particularly in connection with the determination of coordination number. However, the analysis of the experimental data of an alkali halide solution is more complicated than that of the solvent alone for at least two main reasons: (i) the number of atomic pair correlation functions is larger in aqueous solutions and (ii) the resolution of the local

* Corresponding author. E-mail: salah_nasr1@yahoo.fr.
[†] Faculté des Sciences de Monastir.
[‡] Université Tunis- El Manar.
[§] CEA Saclay.

10.1021/jp0641583 CCC: $33.50
Published on Web 10/20/2006

TABLE 1: Values of Lennard-Jones and Electrostatic Interaction Potential Parameters[a]

atom	charge (e)	ϵ (kJ/mol)	σ (Å)
O	−0.82	0.65	3.1656
H	+0.41	0.0	0.0
Na^+	+1	0.544	2.35
Cl^-	−1	0.419	4.4

[a] e represents the magnitude of electronic charge.

order in pure hydrogen-bonded liquids is helped by using the short-range crystalline structure, whereas, in aqueous solutions, the solvent−solvent interactions are generally perturbed and the ion−water interactions lead to "new" signatures which are difficult to be identified only from experimental investigations. MD simulations can provide important information to resolve this problem. This is the approach which we have retained in the present study. We particularly aim to show the possibility of constructing via MD predictions a model of intermolecular arrangement able to describe the local order of our systems as deduced from X-ray data.

To our knowledge, this is the first study where simulated structural results are directly compared with X-ray ones. In section II, we present the simulation methodology and the succinct X-ray formalism theory. In sections III and IV, we respectively describe the experimental procedure and the data treatment. Simulated and experimental results are discussed in section V in terms of water−water, ion−water, and ion−ion pair correlation functions. Particular attention is paid to the induced perturbation on the water H-bond network in relation with salt concentration. According to the characteristics of the first and second hydration shells and the strong electrostatic interactions in solutions as deduced from MD simulation, a model of intermolecular arrangement is proposed to describe the experimental X-ray scattering structure factors. The pair correlation functions constructed from this model are then compared with those extracted from experimental data. The conclusion and final remarks are presented in section VI.

II. Theoretical Considerations

A. Molecular Dynamics Formalism. The MD simulations are carried out on the (NVT) ensemble, at 298 K. At each concentration, the system is made up of 256 molecules including water and ions in a cubic box, to which the length (L) is chosen to match the experimental density described below. For $C = 4$ m, another run with 864 particles is performed to test the possible effect of the system size on simulated results. The weak coupling scheme according to Berendsen et al.,[18] periodic boundary conditions, and minimum image convention are adopted. In all simulations, the water molecules are characterized by the rigid SPC (simple point charge) model[19] while the chloride and sodium ions by the parametrization of Smith et Dang.;[20] all of the intermolecular interactions are expressed as a sum of Coulombic and Lennard-Jones (L-J) 12−6 potentials, that is,

$$U_{ij} = \frac{q_i q_j}{r_{ij}} + 4\epsilon_{ij}\left[\left(\frac{\sigma_{ij}}{r_{ij}}\right)^{12} - \left(\frac{\sigma_{ij}}{r_{ij}}\right)^{6}\right] \quad (1)$$

where σ_{ij} and ϵ_{ij} are obtained by using the Lorentz−Berthelot rules $\sigma_{ij} = (\sigma_i + \sigma_j)/2$ and $\epsilon_{ij} = \sqrt{\epsilon_i \epsilon_j}$. The values of the potential parameters q_i, σ_i, and ϵ_i for all particles are summarized in Table 1.[19,20]

Short-range forces are truncated at the half of the box length, and the Ewald summation technique[21] is employed to treat the long-range Coulomb interaction. The convergence parameter is $\alpha = 5.36/L$ and the maximum k in the reciprocal space is such that $k_{max}^2 \leq 27$. The equations of motion are integrated using the Verlet Leapfrog algorithm,[22] and the method of constraints is applied[23] for the water model. Because of the fast rotation of the water molecules, a 1 fs (10^{-15} s) integration time step is used. All simulations are performed with the computational code MOSCITO.4.

TABLE 2: Simulation Parameters, Experimental Densities, Total Energies, and Standard Deviations of the Studied Systems

	run					
	0	1	2	3	4	5
number of H_2O	256	252	244	230	224	756
number of ions	0	4	12	26	32	108
box length (Å)	19.62	19.56	19.53	19.44	19.41	28.18
simulation time[a] (ns)	3	6	5	4	3.5	3.5
salt concentration (m)	0	0.5	1.5	3	4	4
exptl density (g/cm^3)	1.01	1.018	1.053	1.10	1.128	1.128
E_{tot}/N_{tot} (kJ/mol)	−40.49 (−41.9)	−48.15 (−49.1)	−59.54	−82.51	−90.17 (−91.3)	−90.18
standard deviation	0.13	0.16	0.14	0.13	0.12	0.11

[a] After 500 ps of equilibration. The values in parentheses correspond, respectively, to 0, 0.55, and 4.1 m (ref 5).

We have studied four aqueous sodium chloride solutions at different salt concentrations (0.5, 1.5, 3, and 4 m). For comparison, pure liquid water is also considered. The simulation parameters of the studied systems are reported in Table 2 together with the salt concentrations and the experimental densities. In the starting configuration, the molecules are located at random orientations and the ions randomly distributed in the cubic volume. Initial velocities are generated assuming a Maxwell−Boltzmann distribution, and they are rescaled to guarantee momentum conservation. MD runs of 500 ps are used to equilibrate each system, and then, the simulations are run at least for another 3 ns before the calculation of equilibrium structural quantities. The observation time, the total energy, and the corresponding standard deviation for each system are given in Table 2. Some of the earlier results corresponding to comparable concentrations with the flexible SPC water model and (L-J) interaction potential are also given.[5]

A standard method for studying the structure of solution is to calculate the radial distribution functions between different interaction sites, that is, ion−ion, ion−water, and water−water g_{ij}[24] pair correlation functions. Another characteristic variable is the coordination number (n_{ij}) defined by

$$n_{ij} = 4\pi\rho_j \int_{r_1}^{r_2} r^2 g_{ij(r)}\, dr \quad (2)$$

which gives the mean number of particles (j) contained in a volume defined by two concentric spheres of radii r_1 and r_2 centered on a particle i.

B. X-ray Formalism. The basic theory for X-ray scattering by liquids[25] is well-known, and only a brief outline is given here to describe the local order in our systems. The total structure factor of each solution may be defined as

$$S_M(q) = \frac{\left(\frac{d\sigma}{d\Omega}\right)_{coh}}{\left(\sum_i x_i f_i(q)\right)^2} \quad (3)$$

where q stands for the modulus of the wave vector **q** in the

case of elastic scattering, $(d\sigma/d\Omega)_{coh}$ is the coherent contribution of the differential scattering cross section, and x_i and $f_i(q)$ are, respectively, the atomic fraction and the scattering factor of atom i.

For $q \rightarrow 0$, $\lim S_M(q) = \rho k_B T \chi_T$, where ρ is the molecular number density, k_B is Boltzmann's constant, T is the absolute temperature, and χ_T is the isothermal compressibility. At large q, $S_M(q)$ goes to the asymptotic value

$$S_M(q) = \frac{\sum_i x_i f_i^2(q)}{[\sum_i x_i f_i(q)]^2} \quad (4)$$

The pair correlation function of each system may be deduced as the Fourier transformation of the structure factor $S_M(q)$

$$g(r) = 1 + (2\pi r\rho)^{-1} \int_0^\infty q[S_M(q) - S_M(\infty)] \sin(qr)\, dq \quad (5)$$

III. Experiments

The X-ray diffraction measurements were carried out on a standard $\theta - 2\theta$ diffractometer operating in transmission mode with Mo Kα radiation ($\lambda = 0.7093$ Å) monochromated by a bent asymmetric quartz. The scattered intensity was measured in steps of 0.25° (2θ) in the range 3−55° and in steps of 0.5° at high angles. The maximum q value is 15.34 Å^{-1}. The sample is contained in a flat sample holder (4 mm thick) equipped with Mylar windows. Several scans were done until about 80.000 counts were obtained at each angle. The sodium chloride was supplied by Pharmacopée Européenne (purity >99%) and the solutions were prepared with deionized water.

IV. Data Treatment

Before eq 3 can be used to evaluate the coherent differential scattering cross section, the measured intensities (I_{mes}) were corrected according to the relation[26]

$$I_{corr}(\theta) = [I_{mes}(\theta) - B(\theta)]P(\theta)^{-1} A(\theta)^{-1} G(\theta)^{-1} \quad (6)$$

where $B(\theta)$ is the background correction which is given by the measured scattering of the empty cell and reduced by the transmittance of the liquid, $P(\theta)$ is the polarization factor which is calculated from the expression[27]

$$P(\theta) = \frac{1 + \cos^2 2\theta_0 \cos^2 2\theta}{1 + \cos^2 2\theta} \quad (7)$$

valid in the case when a crystal monochromator with Bragg angle θ_0 is introduced into the beam, $G(\theta)$ and $A(\theta)$ are, respectively, the variation of the effective irradiated volume and the absorption correction. The corrected intensity (I_{corr}) was then transformed from arbitrary to electron units using the following relation

$$I(\theta) = \alpha I_{corr}(\theta) - \sum_i x_i I^i_{incoh}(\theta) \quad (8)$$

where the normalization factor (α) is determined by the Krogh−Moe method[28] and I^i_{incoh} is the incoherent scattering of atom i. The structure factor may be deduced from experimental data by the relation[12]

$$S_M(q) - S_M(\infty) = \frac{\alpha I_{corr}(q) - [\sum_i x_i I^i_{incoh}(q) + \sum_i x_i f_i^2(q)]}{[\sum_i x_i f_i(q)]^2} \quad (9)$$

V. Results and Discussion

The local structure of an electrolyte solution can be conveniently studied by means of water−water, ion−water, and ion−ion pair correlation or radial distribution functions (RDFs). In what follows, we first analyze the behavior of water−water interactions as deduced from MD simulation. Figure 1A shows the oxygen−oxygen pair correlation functions ($g_{OO}(r)$) for different salt concentrations in comparison with that of pure water. For more clarity, the curves are translated by 0.25 along the y axis. Several features of these functions may be addressed:

(i) The first peak is virtually at the same position observed in pure water, that is, 2.77 Å. Simultaneously, the height of this peak is clearly reduced from 2.89 at infinite dilution to 2.26 for 4 m solution. The dramatic decrease of this peak at increasing concentration of Na^+ and Cl^- ions evidently indicates the disruption of the water structure, leading to an increase of the water coordination number, as will be shown below. A similar trend has been observed by Restrepo,[29] Vogel, and Heinzinger[30] who respectively used a restricted/unrestricted SCM and the rigid version of the ST2 water model.

(ii) The location of the second peak, the signature of the so-called tetrahedral structure of water, changes from 4.52 to 4.72 Å and gradually disappears with increasing ion concentration. This phenomenon is similar to that observed in water at elevated temperatures.[31] The presence of ions probably forces the water molecules to occupy the interstitial positions,[32,33] and thus, no well-defined second hydration shell is found around a central water molecule.

(iii) Another significant structural effect of salt concentration is the shifting of the third peak which moves from 6.87 Å for pure water to 6.27 Å for 4 m solution.

The oxygen−hydrogen pair correlation functions ($g_{OH}(r)$) are plotted in Figure 1B. The first and second peaks (respectively at 1.77 and 3.27 Å) are at the same location for all systems. The height of the second peak appears irrelevant to the presence of ions, whereas the amplitude of the first one decreases from 1.48 for pure water to 1.08 for 4 m solution. Such variation, also observed about the first peak in $g_{HH}(r)$ (not represented), may be regarded as the most marked effect of ions on water structure. The diminishing of the first peaks in $g_{OH}(r)$ and $g_{HH}(r)$ is indicative of the decrease in the orientational ordering of a pair of hydrogen-bonded molecules. In fact, the analysis of the running integration numbers reported in Table 3 reveals a clear decrease of the average number of hydrogen bonds per molecule, which moves from 3.8 for infinite dilution to 2.5 for 4 m solution. This result corroborates the recent study of Mountain et al.[34] who used the standard rigid SPC/E water model. Otherwise, the n_{OO} coordination number increases despite the reduction of the first peak height in the $g_{OO}(r)$ curve. This is certainly due to the net shift of the first minimum which moves from about 3.42 Å for pure water to 4.37 for 4 m solution. These conclusions are in quite good agreement with earlier studies.[29,31] However, it is interesting to notice that the description of the first solvation shell is more evident by analyzing the n_{OH} values rather than the n_{OO} ones, since the location of the first valley is not well defined in $g_{OO}(r)$ but remains unaltered in $g_{OH}(r)$.

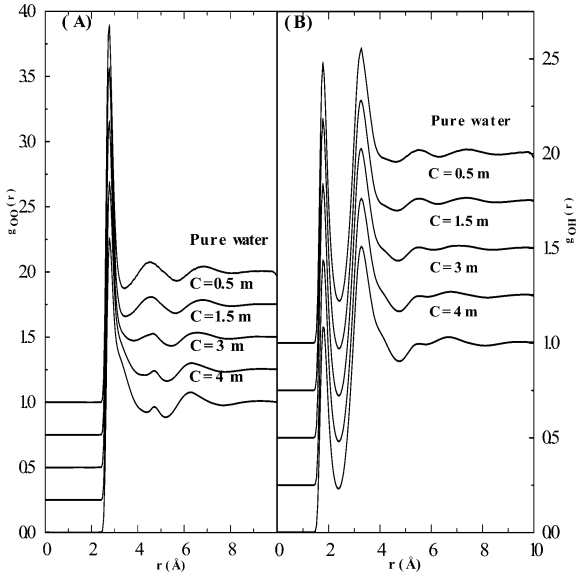

Figure 1. Oxygen−oxygen and oxygen−hydrogen pair correlation functions of aqueous NaCl solutions, compared to the pure water curves, as deduced from MD simulations (A and B, respectively).

TABLE 3: Oxygen−Oxygen (n_{OO}) and Oxygen−Hydrogen (n_{OH}) Coordination Numbers in Aqueous NaCl Solutions at Various Salt Concentrations and at 298 K, as Deduced from MD Simulations

	n_{OO}	n_{OH}
$C = 0$ m	4.53 ± 0.04	3.78 ± 0.05
$C = 0.5$ m	4.92 ± 0.03	3.62 ± 0.02
$C = 1.5$ m	5.85 ± 0.01	3.38 ± 0.01
$C = 3$ m	6.13 ± 0.01	2.86 ± 0.02
$C = 4$ m	6.41 ± 0.01	2.46 ± 0.01

The Na^+ and Cl^-−water pair correlation functions for each concentration are, respectively, displayed in parts A and B of Figure 2. The curves are rather in agreement with previous Guàrdia et al.[35] results, which have used a flexible SPC model; the remaining disagreement with the Dang et al.[36] conclusions about the heights of the peaks should be attributed to the use of nonadditive many body potentials. For the sodium ion, the resulting $g_{NaO}(r)$ distribution functions (Figure 2A, solid line) show two clear solvation shells respectively at 2.37 and about 4.45 Å, related to strong Na^+−O correlations. As the concentration increases, the height of the first peak decreases, leading to a decrease of the coordination number n_{NaO} (see Figure 2A, dotted line) around the first hydration shell. This tendency is particularly in accordance with the study of Lyubartsev et al.[5] using the flexible SPC water model and the recent one of Weerasinghe et al.[37] which have used a Kirkwood−Buff force field (KBFF). Similar trends for $g_{NaH}(r)$ (Figure 2A, dashed line) may be outlined. In other words, the height of the first peak and the n_{NaH} coordination number (not represented) decrease with increasing salt concentration. This is most likely because some water molecules in the first hydration shell are occasionally substituted by chlorine. This effect does not take place in the chlorine hydration, as will be shown below. Finally, it is interesting to mention that, in the $g_{NaH}(r)$ distribution functions, the first peaks lie farther away than the first maximums in the Na^+−O radial distribution functions. This indicates that the oxygen atoms are pointing toward the ion and the hydrogen atoms are facing bulk water.

The $g_{ClO}(r)$ and $g_{ClH}(r)$ pair correlation functions (Figure 2B, solid and dashed lines, respectively) show two first well pronounced peaks at, respectively, 3.22 and 2.27 Å. The calculated chlorine−water hydration numbers (Table 4) do not

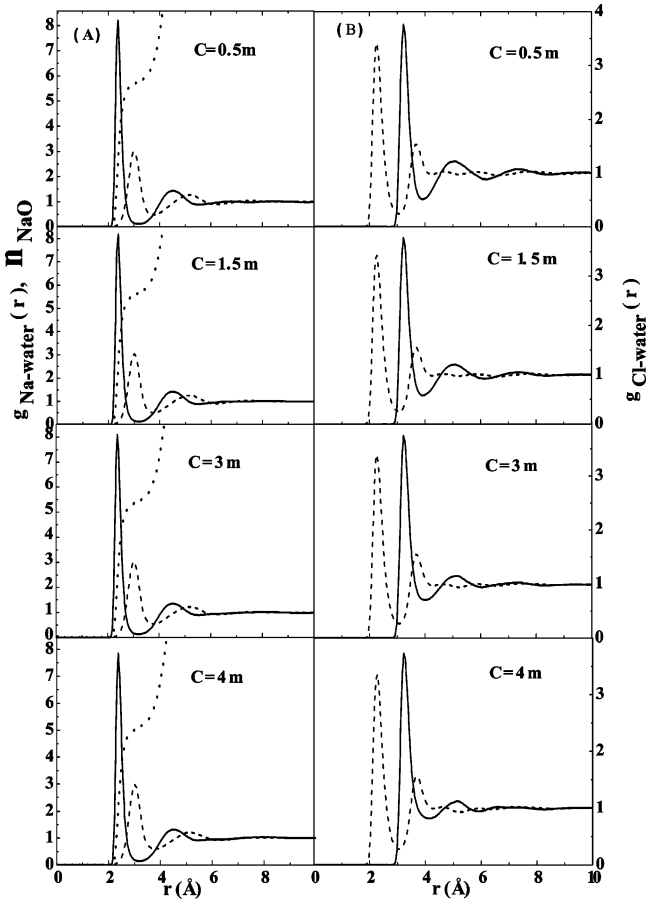

Figure 2. Sodium−oxygen and sodium−hydrogen pair correlation functions of aqueous NaCl solutions (solid and dashed lines, respectively), as deduced from MD simulations. The dotted line represents the n_{NaO} hydration number (A). The chlorine−oxygen and chlorine−hydrogen pair correlation functions of aqueous NaCl solutions (solid and dashed lines, respectively), as deduced from MD simulations (B).

show significant variation with salt concentration. The examination of Cl^-−water radial pair correlation functions show that the hydrogen atoms point toward the Cl^-, whereas the oxygen atoms face bulk water. The fact that the oxygen atom is closest to Na^+ (see above) and the hydrogen atom to Cl^- is due to the charge asymmetry of the water molecule[38] which can be seen in the ion−water distribution functions. In addition to the first peaks, the chlorine−oxygen and chlorine−hydrogen $g_{ij}(r)$ curves show two less pronounced peaks at, respectively, 5.12 and 3.67 Å which are not considerably modified with the salt concentration. Table 4 gives, respectively, the values of the positions r_{M1} and r_{M2} of the first and second peaks of Na^+, Cl^-−water interactions, their corresponding intensities I_{M1} and I_{M2}, and the first hydration numbers H_N. For comparison, similar results deduced from previous studies using different interaction potentials are also quoted.[29,35,36,39−41] Good agreement can be highlighted by comparing our results and corresponding ones from the literature. For example, the Na^+ and Cl^- hydration numbers at 4 m respectively equal to 5.09 and 7.78 are in good agreement with the results of Restrepo et al.[29] (5.10 and 7.9) at 3.95 m using the SCM model with a treatment of ions as charged hard spheres. In the same manner, a quite good concordance is observed between our results at 0.5 m (5.67 and 7.31) and those of Guàrdia et al.[35] (5.7 and 8.4) for dilute solution. Concerning the positions of the first and second maximum in the Na^+, Cl^-−water RDFs, we can also notice a good correspondence between our results and earlier ones, except for minor disagreement in

TABLE 4: Some Characteristics of First and Second Maximums in Na^+−Water and Cl^-−Water Pair Correlation Functions in Aqueous NaCl Solutions, as Deduced from MD Simulations (r_M, Position; I_M, Amplitude; H_N, Hydration Number) (Some Results for Earlier Studies Using Different Interaction Potentials Are Also Quoted for Comparison)

	r_{M1} (Å)	I_{M1}	H_N	r_{M2} (Å)	I_{M2}
		Na^+−O			
$C = 0.5$ m[a]	2.37	8.19	5.67	4.45	1.41
$C = 1.5$ m[a]	2.37 (2.4)	8.16	5.60	4.46	1.38
$C = 3$ m[a]	2.37 (2.4)	8.08	5.43	4.45	1.33
$C = 4$ m[a]	2.37 (2.4)	7.84	5.09	4.46	1.28
ref 29[b]	2.34		5.1		
ref 35[c]	2.325	7.4	5.7		
ref 36[d]	2.35		5.7		
ref 39[e]	2.30		4.28		
ref 40[f]	2.42	5.57	6.95	4.35	
ref 40[g]	2.46	4.86	6.26	4.57	
ref 40[h]	2.43	4.27	5.68	4.57	
ref 41[i]	2.55	6.81 ± 0.36	5.4	4.50	1.37 ± 0.11
		Cl^-−O			
$C = 0.5$ m[a]	3.22	3.88	7.31	5.12	1.24
$C = 1.5$ m[a]	3.22 (3.15)	3.77	7.22	5.12	1.20
$C = 3$ m[a]	3.22 (3.15)	3.74	7.75	5.12	1.17
$C = 4$ m[a]	3.22 (3.15)	3.63	7.78	5.12	1.10
ref 29[b]	3.21		7.9		
ref 35[c]	3.275	3.9	8.4		
ref 36[d]	3.20		6.1		
ref 39[e]	3.45		11.73		
ref 41[i]	3.00	4.22 ± 0.04	7.6	4.95	1.10 ± 0.02
		Na^+−H			
$C = 0.5$ m[a]	3.025	3.13	14.41	5.17	1.24
$C = 1.5$ m[a]	3.025	3.10	14.20	5.17	1.235
$C = 3$ m[a]	3.025	3.04	13.84	5.17	1.22
$C = 4$ m[a]	3.025	2.96	13.23	5.17	1.183
ref 35[c]	3.025	2.7			
ref 36[d]	2.90				
ref 39[e]	3.05		6.97		
ref 40[f]	2.93	2.71			
ref 40[g]	3.04	2.50			
ref 40[h]	2.98	2.27			
ref 41[i]	3.05	3.58 ± 0.0.15	15.6	5.20	1.17 ± 0.04
		Cl^-−H			
$C = 0.5$ m[a]	2.27	3.24	6.719	3.67	1.48
$C = 1.5$ m[a]	2.27	3.29	6.71	3.67	1.52
$C = 3$ m[a]	2.27	3.4	6.79	3.67	1.55
$C = 4$ m[a]	2.27	3.29	6.37	3.67	1.54
ref 35[c]	2.325	3.3			
ref 36[d]	2.20				
ref 39[e]	2.00				
ref 41[i]	2.04	3.06 ± 0.23	5.6	3.29	1.37 ± 0.06

[a] This work, The values in parentheses were deduced from X-ray study. [b] 3.95 molal aqueous NaCl solution, SCM model. [c] Dilute systems, flexible SPC water model, and ion−ion interaction potential deduced from constrained MD simulations. [d] Ion−water clusters, nonadditive many-body potential models. [e] Infinitely dilute system, RISM equations. [f] 512 SPC/E water molecules + Na^+, pure additive model. [g] 512 SPC/E water molecules + Na^+, effective pair model. [h] 512 SPC/E water molecules + Na^+, effective three-body model. [i] 1.791 molal aqueous NaCl solution, flexible/polarizable five-site water model.

the $g_{ClH}(r)$ with refs 39 and 41. However, it is interesting to emphasize that these refs give r_{M1} values lower than all other ones.

In Figure 3, we have drawn the Na−Cl radial distribution functions. The curves have a first maximum at 2.82 Å, a second solvent-separated maximum at 4.98 Å, and a third low maximum at 7.12 Å, typical of strong range electrostatic attraction and short-range soft core repulsion. One can notice the good concordance between these values and those deduced by Lyubartsev et al.[5] who have, respectively, found 2.8, 5.1, and 7 Å. The most noticeable effects of the increase of the salt concentration are a rise of the first maximum and a fall of the second and third ones in the Na−Cl RDFs. This phenomenon of ion pairing between Na^+ and Cl^- which was observed in previous studies is facilitated at much higher temperatures and higher salt concentrations[33,42] because of a decrease in the water dielectric constant. Other studies[31,42,43] related to the equilibrium properties of Na^+ and Cl^- ions in aqueous solutions have suggested, in addition to the ion pairs, triplets and large charged and uncharged clusters of varying size at supercritical temperatures, whereas, in their computational investigations, Degrève et al.[16] have concluded that large ionic clusters stabilized by hydration molecules can be found in aqueous NaCl solution even at room temperature. However, some questions such as the extension, the kinetic of the formation/destructions of the clusters and the fraction of the ions associated in the large clusters remain yet unanswered which clearly illustrated the difficulty of characterizing the local structure in these complex and tricky systems. In agreement with previous studies,[5,44] the first peaks observed in Na^+−Na^+ and Cl^-−Cl^- RDFs (not represented), respectively, at 3.86 and 5.37 Å correspond to a situation where the pair of ions is separated by water molecules. As it has been reported in Table 2, sufficiently long simulations are performed before extracting particularly the ion−ion pair correlation functions. In Table 5, we have reported some characteristics of some RDFs obtained at 1.5 m averaging over several sequential 500 ps pieces of the simulations. One can see that the first maximum of the NaCl RDF is more unstable as compared to the Na−O, Cl−O, and O−O ones. As it is expected, the observed fluctuations are more pronounced in the Na−Cl pair correlation function, the convergence of which is very slow, due to the low statistics of ion pair and their slow diffusion leading to a slow sampling of the configurational space.[5]

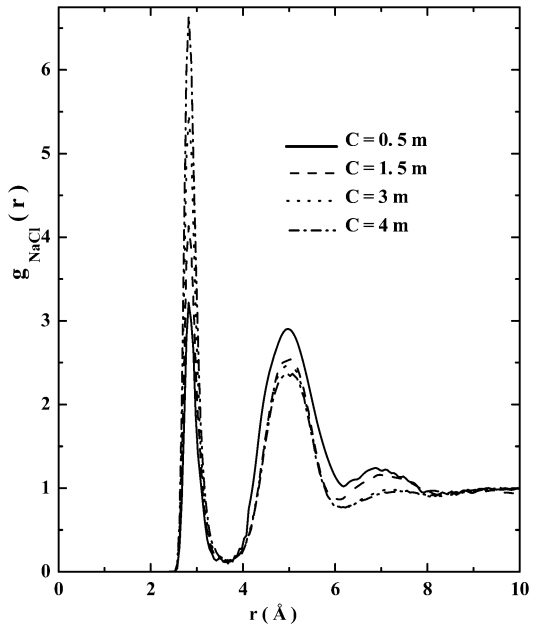

Figure 3. Sodium−chlorine pair correlation functions of aqueous NaCl solutions, as deduced from MD simulations.

As it is mentioned above, some computational studies related to the structural features of aqueous NaCl solutions can be found in the literature. However, the question of local order in these solutions is generally neglected. Moreover, simulated results are not investigated to propose a model of intermolecular arrangement which can be experimentally tested. This is the reason for which we have simultaneously performed X-ray scattering data on the same NaCl solutions previously investi-

TABLE 5: Some Results of 1.5 m Aqueous NaCl Solution, Obtained from Averaging over Several Sequential 500 ps Intervals of the MD Trajectory

	average time (ns)								
	1−1.5	1.5−2	2−2.5	2.5−3	3−3.5	3.5−4	4−4.5	4.5−5	stat error
first maximum of NaCl RDF	4.36	5.12	4.19	3.34	4.46	3.66	3.76	4.18	0.28
second maximum of NaCl RDF	2.88	2.57	2.54	2.49	2.41	2.41	2.52	2.47	0.08
first maximum of NaO RDF	8.24	8.05	8.13	8.18	8.22	8.16	8.17	8.15	0.02
first maximum of ClO RDF	3.91	3.74	3.66	3.71	3.77	3.81	3.79	3.80	0.03
first maximum of OO RDF	2.64	2.68	2.66	2.66	2.66	2.66	2.66	2.66	0.004

gated by MD simulations. We particularly aim at reproducing via MD simulations the local order of solutions as experimentally deduced.

In Figure 4, we have drawn the corrected and normalized intensities ($I_{norm}(q)$) (solid line) for NaCl solutions at different salt concentrations ranging from 0.5 to 4 m and for pure water. The total calculated independent intensities as expressed by $[\sum_i(x_i f_i(q))^2 + x_i I^i_{incoh}(q)]$ are also represented (dashed line) for comparison. We can notice that the experimental and theoretical curves are well superimposed at high q values. The experimental structure factor of each system, deduced from eq 9, is plotted in Figure 5. For a clearer view, the curves are translated by 0.5 in amplitude. We can notice a great similarity between the curves at high q values which indicates that there is no significant variation of the intramolecular water structure when going from pure water to 4 m solution. The ion signature is marked approximately in the 3 $Å^{-1} < q < 8$ $Å^{-1}$ range where the oscillatory character of the curves is amplified with decreasing concentration.

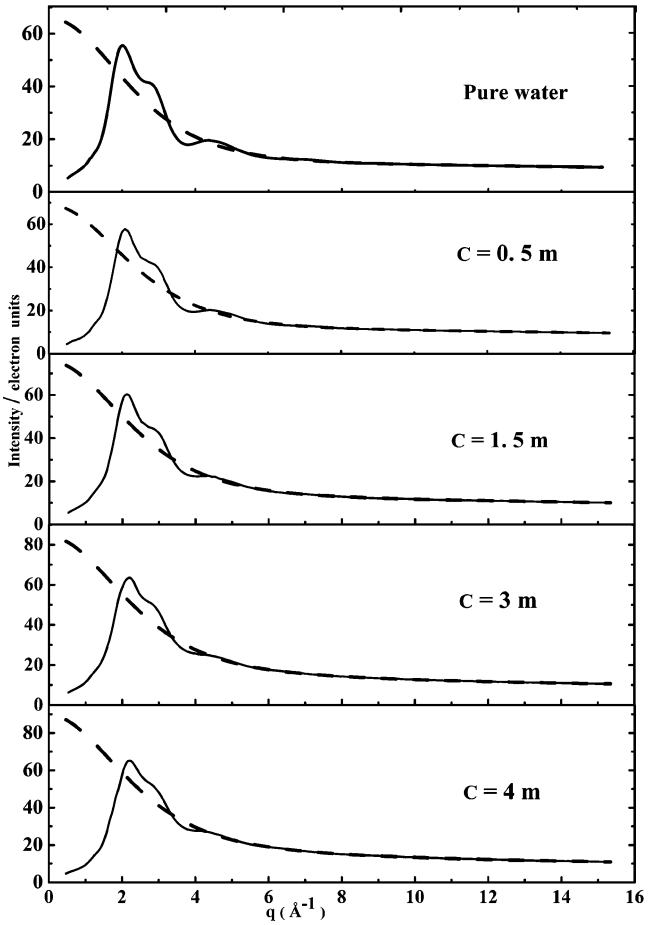

Figure 4. X-ray normalized intensities of aqueous NaCl solutions, compared to the independent intensities $[\sum_i(x_i f_i(q))^2 + x_i I^i_{incoh}(q)]$ (solid and dashed lines, respectively). The pure water curves are also given for comparison.

The salt effect on water structure is easily deduced from X-ray pair correlation functions, derived from the Fourier transformations of the structure factors. In fact, by comparing the solutions and the pure water pair distribution functions (Figure 6), some significant characteristics should be addressed. The curves show at weak concentration (1.5 m) a hump at about 2.4 Å which grows gradually to become a well pronounced peak at higher concentrations (3 and 4 m). According to the MD results, this peak is attributed to the interaction between the cation Na^+ and

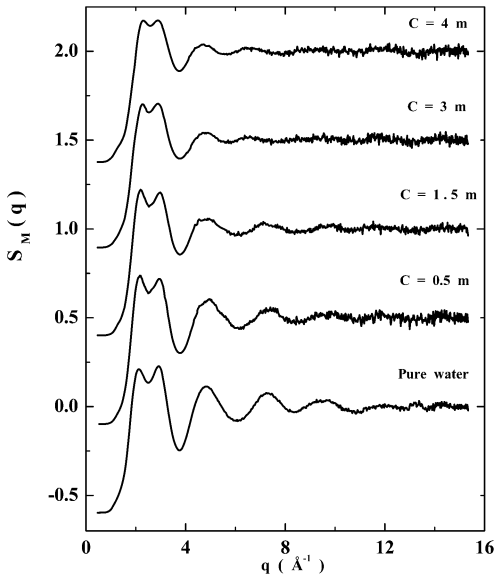

Figure 5. Experimental structure factors of aqueous NaCl solutions at various salt concentrations, compared to the pure water curve.

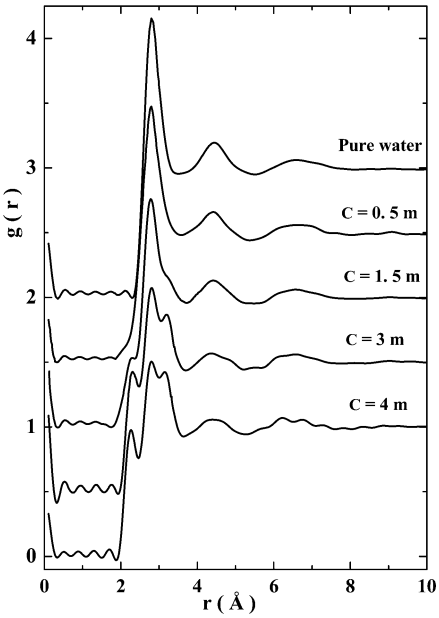

Figure 6. Experimental pair correlation functions of aqueous NaCl solutions, compared to the pure water curve.

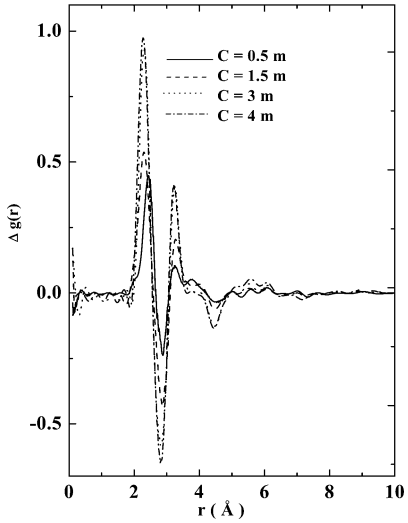

Figure 7. Difference functions, $\Delta g(r) = g_{(NaCl+H_2O)}(r) - g_{H_2O}(r)$, for 0.5, 1.5, 3, and 4 m salt concentrations.

the oxygen atom of water. We also notice the presence of a second distance for ion−water correlation at about 3.15 Å. The development of the Cl^-−O interaction with increasing concentration is evident, since the shoulder observed at 1.5 m is changed into a real peak at 3 and 4 m.

Otherwise, the position of the oxygen−oxygen interaction at about 2.8 Å in the water pair correlation function and which matches well with the results of the pioneer study of Narten et al.[45] appears slightly perturbed by the presence of ions, whereas its height clearly decreases from 2.2 for infinite dilution to 1.51 for 4 m aqueous solution. It is also interesting to observe that this peak is less resolved at raised concentrations and the corresponding first minimum is dramatically shifted in amplitude and in position. This is due to the competitiveness with the Cl^-−O interaction which appears in the vicinity of the O···O interaction. Another marked effect of ions is the progressive weakening of the second peak at 4.5 Å which is the signature of the tetrahedral coordination between water molecules. The pair correlation functions also show other less pronounced maxima which are related to interatomic interactions at higher distances. These features of the total correlation functions may be pointed by representing the difference function $\Delta g(r) = g_{(NaCl+H_2O)}(r) - g_{(H_2O)}(r)$ for each concentration (Figure 7). The ion−water correlations, that is, Na^+−O and Cl^-−O, give rise to two positive peaks, indicating the increase of these interactions with increasing salt concentration. In addition, the well pronounced valleys at 2.8 and 4.5 Å clearly show, as it is described below, the decreases of O−O interactions as the concentration increases.

In the following, we present a model of intermolecular arrangement combining the MD results and X-ray experimental data. To achieve it, some simplifying assumptions have to be considered. The contribution of the X−H (X = O, Na, Cl, H) correlations to the X-ray scattered intensity is weak and sometimes neglected particularly at high q values.[46] Thus, we omit such a term in the theoretical expression of the structure factor. Moreover, we can further assume that there is no significant contribution of Na^+−Na^+ and Cl^-−Cl^- interactions in the pair correlation functions. In fact, no signature of these interactions as deduced by MD simulation, respectively, at 3.86 and 5.37 Å occurs in the experimental curves. This result has also been observed in a recent X-ray study of 1.1 M aqueous NaCl solution.[47] However, we cannot exclude the strong electrostatic attraction between Na^+ and Cl^- that emerges at short distance. Admitting this assumption, we can write

TABLE 6: rms Vibrational Amplitudes (μ_{ij}) and the Interatomic Distances (r_{ij}) as Deduced from the Fitting Procedure (See Text)[a]

$C = 4$ m	$r_{1,ij}$	$\mu_{1,ij}$	$r_{2,ij}$	$\mu_{2,ij}$
Na−O	2.28 (0.04)	0.15	4.53 (0.02)	0.23
Cl−O	3.14 (0.02)	0.19	5.09 (0.01)	0.22
O−O	2.78 (0.01)	0.21	4.46 (0.05)	0.23
Na−Cl	2.79 (0.01)	0.14	5.09 (0.02)	0.23
$C = 3$ m	$r_{1,ij}$	$\mu_{1,ij}$	$r_{2,ij}$	$\mu_{2,ij}$
Na−O	2.31 (0.02)	0.18	4.52 (0.02)	0.24
Cl−O	3.14 (0.02)	0.19	5.10 (0.01)	0.23
O−O	2.79 (0.01)	0.20	4.46 (0.04)	0.24
Na−Cl	2.80 (0.01)	0.13	5.12 (0.03)	0.22
$C = 1.5$ m	$r_{1,ij}$	$\mu_{1,ij}$	$r_{2,ij}$	$\mu_{2,ij}$
Na−O	2.26 (0.05)	0.14	4.52 (0.02)	0.21
Cl−O	3.17 (0.01)	0.21	5.11 (0.01)	0.22
O−O	2.79 (0.01)	0.19	4.45 (0.03)	0.22
Na−Cl	2.81 (0.01)	0.15	5.01 (0.01)	0.23
$C = 0.5$ m	$r_{1,ij}$	$\mu_{1,ij}$	$r_{2,ij}$	$\mu_{2,ij}$
Na−O	2.30 (0.03)	0.18	4.52 (0.02)	0.21
Cl−O	3.14 (0.02)	0.11	4.98 (0.03)	0.25
O−O	2.79 (0.01)	0.21	4.45 (0.03)	0.13
Na−Cl	2.80 (0.01)	0.13	5.10 (0.01)	0.23
pure water	$r_{1,ij}$	$\mu_{1,ij}$	$r_{2,ij}$	$\mu_{2,ij}$
O−O	2.80 (0.01)	0.14	4.45 (0.03)	0.26

[a] The values in parentheses represent the r_{ij} variation in comparison with initial simulated ones.

$$S_M(q) = S_{W-W}(q) + S_{I-W}(q) + S_{I-I}(q) \qquad (10)$$

where $S_{W-W}(q)$, $S_{I-W}(q)$, and $S_{I-I}(q)$ are the partial structure factors, respectively, for water−water, ion−water, and ion−ion aggregates. $S_{i-j}(q)$ is expressed as follows

$$S_{ij}(q) = \frac{x_i x_j f_i(q) f_j(q)}{[\sum_i x_i f_i(q)]^2}\left[\frac{\sin(qr_{1,ij})}{qr_{1,ij}} \exp\left(-\frac{(\mu_{1,ij})^2}{2}q^2\right) + \frac{\sin(qr_{2,ij})}{qr_{2,ij}} \exp\left(-\frac{(\mu_{2,ij})^2}{2}q^2\right)\right] \qquad (11)$$

In this equation, $r_{1,ij}$ and $r_{2,ij}$ are, respectively, the first and the second separation distances between the particles $i-j$ and $\mu_{1,ij}$ and $\mu_{2,ij}$ are the corresponding root-mean-square (rms) vibrational amplitudes for the $i-j$ atom pair or the Debye−Waller (DW) parameters. The computed patterns are estimated according to the two following criteria: (i) by a least-squares fitting of eq 11 to the experimental X-ray structure factors; (ii) by reducing the spurious oscillations of the pair correlation functions at short distances. In this calculation, only the DW parameters are fitted and the bond length variations are fixed within ±5% from MD simulated values. In Table 6, we have reported the values of the optimized r_{ij} distances and the corresponding μ_{ij} parameters.

Despite the crude model used, good agreement is observed between theoretical and experimental X-ray structure factors (Figure 8, dashed and solid lines, respectively) beyond $q = 3$ A^{-1}. Simultaneously, it is worth mentioning that the mean features of the experimental pair correlation functions (Figure

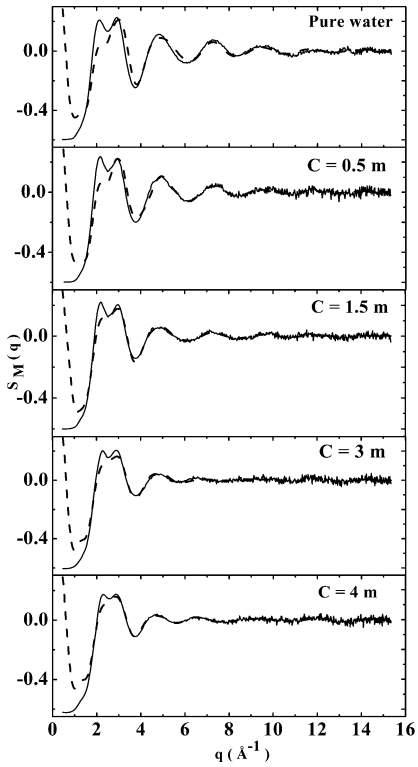

Figure 8. X-ray structure factors of aqueous NaCl solutions and of pure water, compared to the computed patterns deduced from MD simulations (solid and dashed lines, respectively).

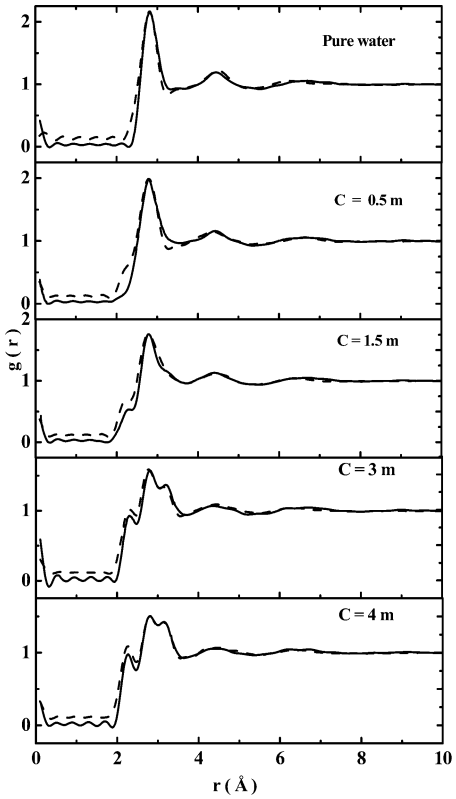

Figure 9. X-ray pair correlation functions of aqueous NaCl solutions and of pure water, compared to the theoretical ones (solid and dashed lines, respectively).

9, solid line) are reproduced by the computed ones (dashed line). Particularly, the first four peaks in the experimental curves respectively assigned to Na^+-O, first O−O, Cl^-O and second O−O interactions are well accounted for by the proposed model.

VI. Conclusion

To determine the local order in aqueous solutions is obviously a more complicated task than to study the solvent alone. For a simple salt of type MX in H_2O, there are 10 different interactions to identify. Aside from the X−H correlations which may be neglected in the X-ray scattering, four pair correlation functions are to be identified, that is, M−O, X−O, O−O, and M−X. Molecular dynamics simulations can help to resolve a feature in the structural information for diffraction experiments. This is the approach which we have adopted in this paper.

Both simulated and experimental results show that the presence of ions produces a perturbation in the association structure of the solvent. Significant changes are observed in the oxygen−oxygen, oxygen−hydrogen, and hydrogen−hydrogen pair correlation functions. As the salt concentration increases, the local water structure is broken down to force molecules to occupy interstitial positions and, as a result, no well-defined second hydration shell is found around a central molecule. The degree of hydrogen bonding in liquid water clearly decreases, whereas the coordination number of water in solution increases if compared to that of the pure fluid. In this respect, the increase of the salt concentration has a similar effect on water as the increase of temperature.

The basic feature in ionic solutions is then the perturbation of water−hydrogen bonds and the appearance of electrostatic interactions between ions and water. Both cations and anions are dissolved by water molecules at the expense of the break down in the hydrogen-bonded water molecules. Using the rigid SPC model, it has been found that the Na^+ hydration number decreases with increasing salt concentration, whereas no significant variation in the Cl^- hydration numbers is observed.

The NaCl partial RDFs show that, with increasing salt concentration, the probability of contact ions also increases and that of solvent-separated ion pair formation decreases. The increase of salt concentration seems to have a similar effect to that observed with increasing temperature. In fact, at room temperature, water molecules tend to form hydrogen bonds, further shielding the interactions between ions, but at increased temperature, the hydrogen bond network of water molecules breaks down, leading to a significant attraction between Na^+ and Cl^-.

According to the MD simulation results, a model of intermolecular arrangement is proposed to describe the experimental data. The computed patterns, mainly based on O−O, Na^+-O, Cl^-O, and Na^+-Cl^- interactions, fairly agree with the X-ray structure factors. Moreover, the main features of the experimental pair correlation functions are accounted for by the proposed model.

To get further insight into NaCl aqueous solution properties, neutron scattering experiments and MD simulation study under nonambient conditions are in progress.

Acknowledgment. The authors would like to thank Nabiha Bchir and Fethi Jenzri for helping them to improve the language of their paper.

References and Notes

(1) Xu, H.; Berne, B. J. *J. Phys. Chem. B* **2001**, *105*, 11929.

(2) Levitt, M.; Hirshberg, M.; Sharon R.; Laidig, K. E.; Daggett, V. *J. Phys. Chem. B* **1997**, *101*, 5051.

(3) Jeffery, G. A.; Saenger, W. *Hydrogen Bonding in Biological Structures*; Springer-Verlag: Berlin, 1991.

(4) Koneshan, S.; Rasaiah, J. C.; Lynden-Bell, R. M.; Lee, S. H. *J. Phys. Chem. B* **1998**, *102*, 4193.

(5) Lyubartsev, A. P.; Laaksonen, A. *J. Phys. Chem.* **1996**, *100*, 16410.

(6) Pitera, Jed W.; van Gunsteren, Wilfred F. *J. Am. Chem. Soc*. **2001**, *123*, 3163.
(7) Jayaram, B.; Beveridge, D. L. *J. Phys. Chem.* **1991**, *95*, 2506.
(8) Zhou, J.; Lu, X.; Wang, Y.; Shi, J. *Fluid Phase Equilib*. **2002**, *194*−*197*, 257.
(9) Lawrence, R. M.; Kruh, R. F. *J. Chem. Phys*. **1967**, *47*, 4758.
(10) Licheri, G.; Piccaluga, G.; Pinna, G. *J. Appl. Crystallogr*. **1973**, *6*, 392.
(11) Narten, A. H.; Vaslow, F.; Levy, H. A. *J. Chem. Phys.* **1973**, *58*, 5017.
(12) Pálinkás, G.; Radnai, T.; Hajdu, F. *Z. Naturforsch.* **1980**, *35A*, 107.
(13) Liu, W.; Sakane, S.; Wood, R. H.; Doren, D. J. *J. Phys. Chem. A* **2002**, *106*, 1409.
(14) Grossfield, A.; Ren, P.; Ponder, J. W. *J. Am. Chem. Soc*. **2003**, *125*, 15671.
(15) Belch. A. C.; Berkowitz. M.; McCammon, A. *J. Am. Chem. Soc.* **1986**, *108*, 1755.
(16) Degrève, L.; da Silva. F. L. B. *J. Mol. Liq*. **2000**, *87*, 217.
(17) Degrève, L.; da Silva. F. L. B. J. *Chem. Phys*. **1999**, *111*, 5150.
(18) Berendsen, H. J. C.; Postma, J. P. M.; Van Gunsteren, W. F.; DiNola, A.; Haak, J. R. *J. Chem. Phys*. **1984**, *81*, 3684.
(19) Berendsen, H. J. C.; Postma, J. P. M.; van Gunsteren, W. F.; Hermans, J. In *Intermolecular Forces*; Pullman, B., Ed.; Reidel: Dordrecht, The Netherlands, 1981.
(20) Smith, D. E.; Dang, L. X. *J. Chem. Phys*. **1994**, *100*, 3757.
(21) de Leeuw, S. W.; Perram, J. W.; Smith, E. R. *Proc. R. Soc. London.* **1980**, *373A*, 27.
(22) Verlet, L. *Phys. Rev*. **1967**, *159*, 98.
(23) Ryckaert, J.-P.; Ciccotti, G.; Berendsen, H. J. C. *J. Comput. Phys.* **1997**, *23*, 327.
(24) Ohtaki, H.; Fukushima, N. *Pure Appl. Chem.* **1991**, *63*, 1743.
(25) Bertagnolli, H.; Chieux, P.; Zeidler, M. D. *Mol. Phys.* **1976**, *22*, 759.
(26) Nasr, S.; Ghèdira, M.; Cortès, R. *J. Chem. Phys*. **1999**, *110*, 10487.
(27) Bertagnolli, H.; Zeidler, M. D. *Mol. Phys*. **1987**, *35*, 177.
(28) Krogh-Moe, J. *Acta Crystallogr*. **1956**, *9*, 951.
(29) Llano-Restrepo, M.; Chapman, W. G. *J. Chem. Phys.* **1994**, *100*, 8321.
(30) Vogel, P. C.; Heinzinger, K. *Z. Naturforsch*. **1976**, *31A*, 476.
(31) Koneshan, S.; Rasaiah, J. C. *J. Chem. Phys.* **2000**, *113*, 8125.
(32) Chowdhuri, S.; Chandra, A. *J. Chem. Phys*. **2001**, *115*, 3732.
(33) Sherman, D. M.; Collings, M. D. *Geochem. Trans*. **2002**, *3*, 102.
(34) Mountain, R. D.; Thirumalai, D. *J. Phys. Chem. B* **2004**, *108*, 19711.
(35) Guàrdia, E.; Ray, R.; Padró, J. A. *J. Chem. Phys.* **1991**, *95*, 2823.
(36) Dang, L. X.; Rice, J. E.; Caldwell, J.; Kollman, P. A. *J. Am. Chem. Soc.* **1991**, *113*, 2481.
(37) Weerasinghe, S.; Smith, P. E. *J. Chem. Phys.* **2003**, *119*, 11342.
(38) Rasaiah, J.; Lynden-Bell, R. *Philos. Trans R. Soc*. **2001**, *359*, 1545.
(39) Pettit, B. M.; Rossky, P. J. *J. Chem. Phys.* **1986**, *84*, 5836.
(40) Spangberg, D.; Hermansson, K. *J. Chem. Phys*. **2004**, *120*, 4829.
(41) Zhu. S.-B.; Robinson, G. W. *J. Chem. Phys*. **1992**, *97*, 4336.
(42) Driesner, T.; Seware, T. M.; Tironi, I. G. *Geochim. Cosmochim. Acta* **1998**, *62*, 3095.
(43) Tester, J. W.; Marrone, P. A.; DiPippo, M. M.; Sako, K.; Reagan, M. T.; Arias, T.; Peters. W. A. *J. Supercrit. Fluids* **1998**, *13*, 255.
(44) Uchida, H.; Matsuoka, M. *Fluid Phase Equilib*. **2004**, *219*, 49.
(45) Narten, A. H.; Levy, H. A. *J. Chem. Phys.* **1971**, *55*, 2263.
(46) Hammami, F.; Nasr, S.; Bellissent-Funel, M.-C.; Oumezzine, M. *J. Phys. Chem. B* **2005**, *109*, 16169.
(47) Okhulkov, A. V.; Gorbaty, Y. E. *J. Mol. Liq.* **2001**, *93*, 39.